SAND2017-12073C

ON THE SENSITIVITY OF ENERGY METRICS TO FAILURE IN A COMPLEX STRUCTURE

Vit Babuška, Carl Sisemore, Jason Booher
Sandia National Laboratories[1]
Albuquerque, New Mexico

System operating environments are frequently only understood in an average or nominal sense and the exact operating environment for any given component can vary sometimes substantially. For this reason, systems and components are designed conservatively. That additional conservatism in the design provides for margin to withstand unexpected operating environment and exposure duration changes. It is common for component designs to be qualified to +6dB above the maximum predicted environment (MPE) with additional exposure duration of three or more expected lifetimes. As a result, components are frequently more robust than the environment demands.

Most qualification programs test to a predefined qualification spectrum for a predefined time. If additional margin is required, then the qualification spectrum is linearly increased—input RMS level for vibration tests and Shock Response Spectra (SRS) for shock tests. If additional exposure duration margin is needed then the test time is increased by some factor while the spectrum remains fixed. As a result, qualification programs may not explore the environment space consisting of exposure levels, exposure durations, and spectral content. Spectral content changes are typically completely ignored in margin test methodology. Inherent in this focus on input level and duration is an assumption that the component failure mode does not change with environmental changes. This assumption may hold true in regimes near the qualification level; however, the assumption is certainly not universally true. This is obvious in the extreme where a cyclic loading at some nominal level results in component failure due to high-cycle fatigue. If the level is increased, it will be possible to move from the high-cycle fatigue regime to the low-cycle fatigue regime. If the level is further increased, it will at some point be possible to fail the component on the first half-cycle.

This work focuses on quantifying a structure's functional capability outside the qualification environments. The methodology proposed here is based on energy spectrum and modal energy since energy is sensitive to the failure mode. A simple test structure was designed and manufactured using additive manufacturing to investigate and demonstrate the functional relationships. The structure on which the work is demonstrated is a platform with structural appendages. The appendages are designed to each have multiple failure modes. The excitation level, duration, and spectral content are varied to exercise different failure modes, and the energies to failure are compared.

ENERGY QUANTITIES OF INTEREST

The equation of motion of a linear SDOF oscillator subjected to a prescribed base acceleration is:

$$\ddot{v}(t) + 2\zeta\Omega\dot{v}(t) + \Omega^2 v(t) = -\ddot{z}(t) \tag{1}$$

where $2\zeta\Omega = \frac{c}{m}$, and $\Omega^2 = \frac{k}{m}$, and $w(t)$ is the relative displacement of the mass to the base, i.e., $v(t) = x(t) - z(t)$. The initial conditions at $t = 0$ are $v(0) = v_0$, and $\dot{v}(0) = \dot{v}_0$. The equation of motion is paired with an output equation that defines the response quantities in terms of the states, $\big(v(t), \dot{v}(t)\big)$. The general form of the output equation is:

$$y(t) = g(v(t), \dot{v}(t), \ddot{z}(t)) \tag{2}$$

Typical response quantities are absolute acceleration, relative displacement, $v(t)$, and relative velocity, $\dot{v}(t)$, and/or functions thereof. The output equation can be a vector equation when more than one response quantity is of interest. In this

---

[1] Sandia National Laboratories is a multi-mission laboratory managed and operated by National Technology and Engineering Solutions of Sandia, LLC., a wholly owned subsidiary of Honeywell International, Inc., for the U.S. Department of Energy's National Nuclear Security Administration under contract DE-NA0003525.

paper, we are interested in specific energy (i.e., energy per unit mass) quantities, which are derived by integration of equation 1 with respect to x. Upon integration, a three-term decomposition of the total energy is obtained.

$$\tilde{E}_K(t) + \tilde{E}_D(t) + \tilde{E}_A(t) = \tilde{E}_I(t) \quad (3)$$

Equation (3) is the energy balance relation described by Zahrah and Hall [1, 2] in their derivation of earthquake energy relationships. The energy balance equation is of interest because it shows the relationships between the energy terms. The values of the energy quantities are obtained from the states of the SDOF oscillator equation of motion. In this work, two energy quantities are of interest: Steady state specific input energy and peak specific absorbed energy. The specific input energy of a linear SDOF oscillator is:

$$\tilde{E}_I(t) = -\int_0^t \dot{v}(\tau)\ddot{z}(\tau)d\tau\,, \qquad 0 < t \leq T \quad (4)$$

where T is the duration of the base excitation. The specific absorbed energy,

$$\tilde{E}_A(t) = \frac{1}{2}\Omega^2[v^2(t) - v^2(0)],\ \ 0 < t \leq T \quad (5)$$

Specific input energy is of interest because it quantifies velocity based dissipation independent of a model. It can be calculated in the time domain with Eq. (4), or in the frequency domain by applying Parseval's theorem to Eq. (4) with $t = T$, and recognizing that

$$\dot{V}(j\omega) = \frac{-j\omega}{\Omega^2 - \omega^2 + j2\zeta\Omega\omega}\ddot{Z}(j\omega) = G(j\omega)\ddot{Z}(j\omega) \quad (6)$$

where $\ddot{Z}(j\omega, T)$ is the finite Fourier transform of the base acceleration. The result is:

$$\tilde{E}_I(T) = -\frac{1}{\pi}\int_0^\infty Re[G(j\omega)]\left|\ddot{Z}(j\omega, T)\right|^2 d\omega \quad (7)$$

because $\ddot{Z}(j\omega)$ has Hermitian symmetry so $\left|\ddot{Z}(j\omega, T)\right|^2$ is real, and the imaginary part of $G(j\omega)$ is odd so it's integral evaluates to zero.

The peak absorbed specific energy $\tilde{E}_{A_M}$ represents the extreme response associated with a first passage type failure. It is calculated from the response spectrum in the time domain:

$$\tilde{E}_{A_M}(\Omega, \zeta) = \|E_A\|_\infty = \max_t\left|\tilde{E}_A(t, \zeta, \Omega)\right|\ \ \forall\, \zeta, \omega;\ 0 \leq t \leq T \quad (8)$$

In this work, we compute the absorbed energy spectrum using the acceleration measured on a component of interest rather than on the base acceleration.

TESTING OVERVIEW AND RESULTS

The test platform and the appendages were all made of ABS by the Sandia National Laboratories Additive Manufacturing group. The components were easily made and relatively inexpensive, allowing for multiple tests. A photograph of one of the plate structures is shown in Fig. 1. The 5-inch square plate was supported at two opposing corners as shown using printed circuit board standoffs. The plate's two halves were designed with different thicknesses to give differing resonant frequencies on each side. Three styles of appendages are shown in Fig. 1. The collars added to the appendages carried accelerometers but also served to add significant mass to the appendages to increase the stress within each sub-component. Each appendage includes a stress concentration zone so that failure is consistent.

Shock testing was performed on a drop table at the Sandia National Laboratories Mechanical Shock Laboratory. Testing was performed in several series. Initial testing focused on increasing the shock level to establish failure points for the various platform appendages. After this, low-cycle fatigue testing to failure was performed to establish failure versus number of shock curves. Testing was also performed at differing shock pulse durations to alter the spectral content of the applied shock loading. Only the 5 msec tests are considered in this paper.

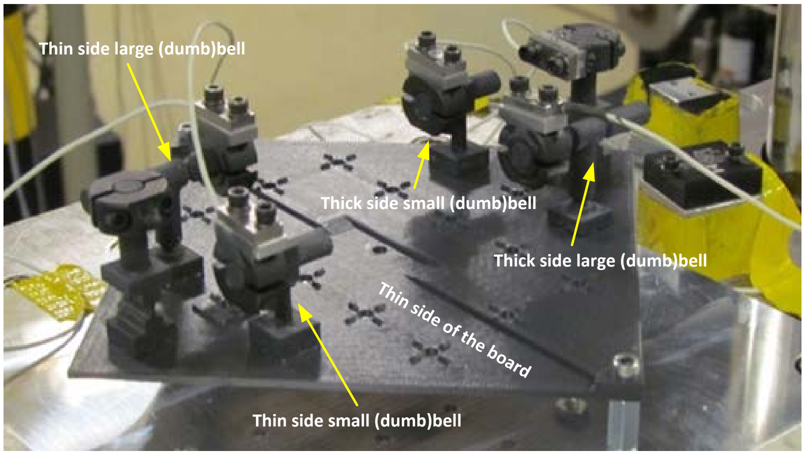

Fig. 1 Test Platform with Six Appendages Installed Ready for Shock Testing

To understand trends in the quantities of interest and the correlation between input energy and structural failure, as well as the correlation between absorbed energy and structural failure, many drop tests were performed on nominally identical structures, only a few of which are considered here. Table 1 summarizes some of the test conditions. The baseline environment for the test structure was a 40 G 5 msec Haversine shock.

Table 1 Sampling of Shock Environments

Test Number	Peak G	Duration (ms)	Comments
149	39	5.2	Baseline Environment
157	59	4.9	Nothing broke
150	58	4.9	Nothing broke
156	58	4.9	Thick side tower broke (not instrumented)
154	100	5.2	Thin side small bell broke

Fig. 2(a) shows the specific input energy of four components on the board at the baseline environment, and Fig. 2 (b) shows the absorbed energy response spectra for the four components. The resonant responses are obvious in Fig. 2 (b). Fig. 3 summarizes the steady state specific input energy and the peak values in the absorbed energy spectra at the four shock amplitudes at each component. The thin side small bell consistently had the lowest absorbed energy of the four components, yet it was the one that failed on the 100 G shock. The thin side large bell showed a much larger increase in absorbed energy at the 100G level than the other components. Neither the input energy nor the absorbed energy show a squared relationship to input amplitude suggesting that the structure is nonlinear.

Fig. 4 shows test to test variation for 60 G shocks. The variability in input energy was lower than absorbed energy variability. The average input energy was highest at the large bell on the thick side, but the absorbed energy was greatest at the small bell on the thick side. The absorbed energy of small bell on the thin side was clearly the lowest of the four components, but the input energy of the thin side small bell was comparable to that of the other components.

CONCLUSIONS

Input energy and absorbed energy were investigated to understand their usefulness as quantities to describe shock environment and response severity. Both spatial and amplitude variations were considered. Neither the specific input energy nor the specific absorbed energy scaled proportionally with shock amplitude squared suggesting that the test structure is non-linear.

REFERENCES

1. Zahrah, T. F. and Hall, W. J., “Earthquake Energy Absorption in SDOF Structures,” *Journal of Structural Engineering*, Vol. 110, No. 8, August 1984, pp. 1757–1772.
2. Zahrah, T. F. and Hall, W. J., “Seismic Energy Absorption in Simple Structures,” *Civil Engineering Studies, Structural Research Series No. 501*, University of Illinois, Urbana, Illinois, July 1982.

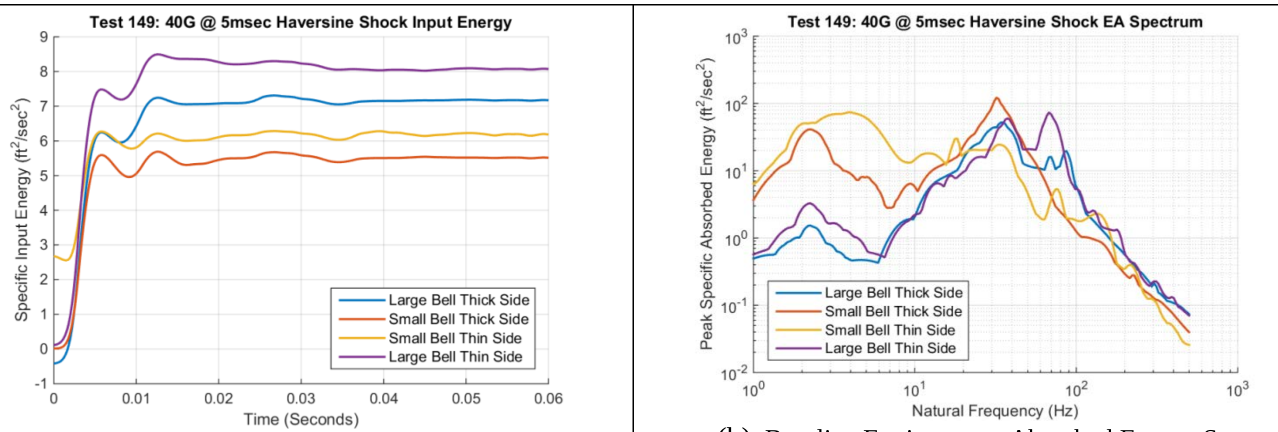

(a) Input Energies in the Baseline Environment (b) Baseline Environment Absorbed Energy Spectra

Fig. 2 Input Energies and Absorbed Energy Spectra in the Baseline Environment

EI (ft^2/sec^2)					
		Component			
Test	Peak G	Large Bell Thick Side	Small Bell Thick Side	Small Bell Thin Side	Large Bell Thin Side
149	40	6.6	4.4	3.4	7.3
157	60	18.0	14.7	15.8	13.2
150	60	18.5	16.8	14.6	17.5
156	60	17.4	13.4	15.0	13.1
154	100	47.7	51.6	3.2	34.9

(a) Specific Input Energy

EA (ft^2/sec^2)					
		Component			
Test	Peak G	Large Bell Thick Side	Small Bell Thick Side	Small Bell Thin Side	Large Bell Thin Side
149	40	52.4	121.9	73.9	73.4
157	60	217.4	210.3	91.1	168.7
150	60	153.3	174.2	93.6	190.3
156	60	264.2	304.9	111.0	145.2
154	100	343.1	373.6	0.0	660.0

(b) Specific Absorbed Energy

Fig. 3 Specific Input Energy and Absorbed Energy at 4 Shock Levels

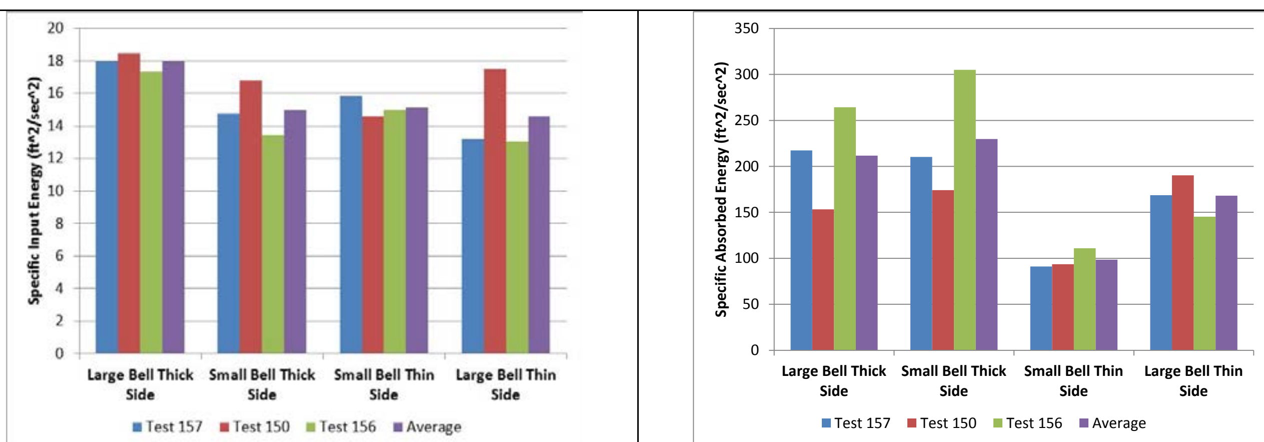

(a) Specific Input Energy for 60 G Shocks (b) Specific Absorbed Energy for 60 G Shocks

Fig. 4 Specific Input Energy and Absorbed Energy for 3 60 G Shocks